A Module-Based Plug-n-Play DC Microgrid With Fully Decentralized Control for IEEE Empower a Billion Lives Competition

Dong Li, *Student Member, IEEE*, and Carl Ngai Man Ho, *Senior Member, IEEE*

***Abstract*—In this article, a module-based plug-n-play (PnP) dc microgrid (MG) is introduced to help rural electrification. It provides a bottom-up way to form an MG with multilayer expandability and PnP feature. The module-based MG overcomes the drawback of conventional MG that requires central design and implementation which leads to high upfront cost and long lead time. It provides an organic way to form an MG that allows user to scale up the system as their demands grow, and fully utilize the existing resources. The proposed MG module is expandable on different layers that can meet the requirements of customers with different power consumption requirements. Each module, which contains PV generation and energy storage, can work as a stand-alone solar home system. Multiple modules can be connected as a group to scale up the local power supply. Groups can be interconnected through a public bus with gateway converter modules to form a community network, which can supply public usage and enable power exchange in a community range with relatively high distribution efficiency. The control of the proposed MG is in a fully decentralized manner such that central control and communication network can be omitted, which makes the system more user-friendly and highly robust. Detailed design, analysis, and implementation of the proposed PnP MG is provided in this article. Simulation and experimental results have been provided to verify the concept and analytical study.**

***Index Terms*—DC microgrid (MG), modular MG, MG module, decentralized control, rural electrification.**

NOMENCLATURE

BES	Battery energy storage.
GC	Gateway converter.
MG	Microgrid.
MPP	Maximum power point.
MPPT	Maximum power point tracking.
PnP	Plug-and-play.
PU	Power unit.
PV	Photovoltaic.
SHS	Solar home system.
SoC	State of charge.

Manuscript received May 11, 2020; revised June 12, 2020; accepted July 9, 2020. Date of publication July 15, 2020; date of current version September 22, 2020. Recommended for publication by Associate Editor C. K. Tse. This work was supported by the Canada Research Chairs under Grant Sponsor ID: 950-230361. This article was presented in part at the IEEE Empower a Billion Lives Competition as an emerging technical solution by the team "Winnie the Power" and was awarded the "Best Student Team Award of Americas Region." *(Corresponding author: Dong Li.)*

The authors are with the Department of Electrical and Computer Engineering, University of Manitoba, Winnipeg, MB R3T 2N2, Canada (e-mail: lid34514@myumanitoba.ca; carl.ho@umanitoba.ca).

Color versions of one or more of the figures in this article are available online at https://ieeexplore.ieee.org.

Digital Object Identifier 10.1109/TPEL.2020.3009631

I. INTRODUCTION

ACCORDING to International Energy Agency, over 3 billion people are living in energy poverty and more than 1 billion people are living with no access to electricity [1]. It has been a challenge to develop new ways to power up these unelectrified areas. The high cost and geographical limitations in most of the unelectrified areas make the conventional power system, which relies on central generation and long-distance transmission, no longer effective to solve the current energy poverty problem [2], [3]. Meanwhile, powering up billions of people with conventional fuel-burn plants could generate giga tons more of carbon emission. Alternatively, photovoltaic (PV) based off-grid dc microgrid (MG) systems have been developed with new business models to make electricity affordable to households in energy poverty areas [2].

Most of the less-electrified regions are in Africa and South Asia, which are rich in solar resources. This makes solar PV generation a competitive way toward conventional generation. The distributed character of PV generation relies on MG as an effective way to utilize solar energy [4]–[7]. MG integrates generation, load, and energy storage, which can constantly provide relatively high power and support a variety of loads. However, the common approach to build an MG requires a centralized design, installation, and operation. As a result of this top-down approach, professionals are required, the cost (including design, installation, and operation) are increased, the lead time is prolonged, and the future expansion of MG is difficult. With the conventional approach, the MG capacity will be overdesigned or insufficient most of time due to the difficulty of expanding. And it is hard for people living in energy poverty to raise money for the upfront investment. These drawbacks are strangling the development of MG in rural areas.

To overcome the drawbacks of conventional central MG by making MG plug-and-play (PnP) to be easily scaled up, more and more research on flexible MG structures, modular MGs, and MG clusters have been proposed [8]–[11]. In [12], few major concerns to achieve PnP in MG system have been pointed out, among which, the most important is how to avoid communication which may spoil the scalability and reduce system reliability and how to design a decentralized control

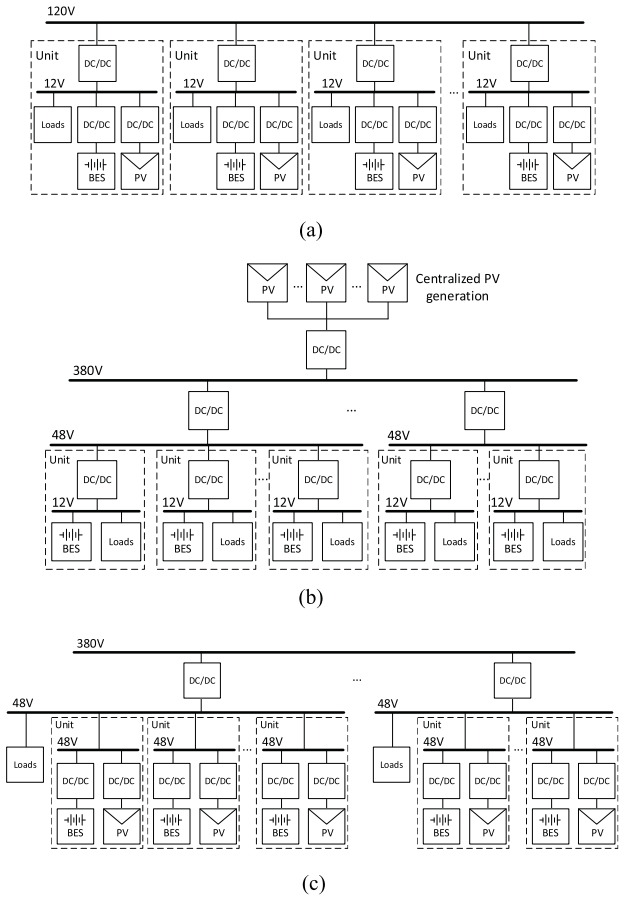

Fig. 1. Prior art and proposed scalable MG structures. (a) Scalable MG structure used in [13]–[15], [17]. (b) Scalable MG structure proposed in [16]. (c) PnP MG proposed by this article.

system independent of the total number of modules to achieve a real scalable design. In [13] and [14], distributed control technologies based on peer-to-peer communication have been studied. In [13], an open energy system that allows independent nanogrids to be interconnected as an MG has been proposed, which relies on a peer-to-peer control system. Similarly, [14] has proposed a distributed cooperative control system. Though the central controller is eliminated, the systems still rely highly on communication network, which may not be preferred in a rural application where communication could increase the cost and reduce the reliability as well as the scalability. In [15]–[17], decentralized solutions have been provided where the MG system can become independent of communication and realize PnP. In [15], a scalable MG architecture based on droop control has been proposed that relies only on local information, which is highly suitable for rural electrification. In [16], a scalable MG with centralized generation and decentralized home power management units (PMUs) has been proposed. In [17], a self-organizing nanogrid (SONG) system has been proposed, which is based on a low-cost multiport converter unit.

Fig. 1(a) shows a typical structure of scalable MG. Most prior arts of scalable MG are based on this general structure, where the control, topology, and scale may vary in different projects. The expansion is based on a dc–dc converter as an interface of each unit. The advantage of this structure is the simple control that each unit is isolated by the interfacing dc–dc converter and just needs to manage power balance of its own. However, the disadvantage is also obvious. First, since the house load is connected to local bus, the available power to the load is limited by the rating of interfacing dc–dc converter regardless of the number of units. Second, when power goes from one unit to another unit, it needs to go through the interfacing converter two times, which could be lossy.

Fig. 1(b) shows the scalable MG structure used in [11]. Instead of having PV modules in each unit, this structure has a centralized PV generation. The PMUs installed at each user only contain battery energy storage (BES) and loads. Thus, the control of each unit can be significantly simplified without local generation. The available power on the 12-V bus is also limited by the single converter capacity. Power on the 48-V cluster bus is scalable. However, due to the centralized generation, the modularity is reduced so that a single unit cannot work without generation, and it is economically viable only for relatively large communities.

Fig. 1(c) shows the proposed PnP MG structure. First, in this structure, each unit has BES and PV generation which can be used as a stand-alone unit. Second, since the connection of multiple units uses the local bus directly without any interfacing converters, the power on the 48-V bus is scalable without single converter limit and the loss is reduced without interfacing converters. Third, to interconnect multiple groups, an interface converter, otherwise called a gateway converter (GC), is used to create a relatively high voltage distribution network.

As shown in Fig. 1(c), the proposed MG has three expansion layers. First, a single power unit (PU) can work as a stand-alone SHS. Each PU contains PV generation and BES with a common 48 V dc bus as output. Second, multiple PUs can be interconnected directly with the 48-V local dc bus as a group. Third, multiple groups can be connected to a public dc link (200–400 V), through GC. Intergroup expansion is at community level and allows power exchange among households and pooling power for public usages.

Conventionally, for central-planned commercial dc MG, communication-based hierarchical control structure is commonly used [18]–[20]. The involvement of control center and communication network significantly reduces system modularity. To better introduce PnP into MG, the study on decentralized control became popular. In the literature, [13], [14], and [21]–[23] studied decentralized control of MG. Though the central controller is removed, they still rely on the communication network. Most of the studies on communicationless control of MG only focus on primary control and system stability [24]–[26], while some other important aspects of MG control, e.g., state-of-charge (SoC) balancing and control mode selection, are overlooked. In this article, to keep a high modularity and reliability, a fully decentralized and communicationless control is applied to the proposed MG system. The direct bus connection inside a group increases the difficulty of coordinating all the parallel BES converters and parallel PV converters. It is challenging to achieve power sharing, BES SoC balancing, PV-BES coordination, and intergroup coordination at the same time in a

communicationless manner. The proposed control is based on modified droop control, of which, the stability is as good as common droop-controlled systems. With the proposed control methods, units can be bus interfaced with a well-designed droop control system based on dc bus signaling technology [27]–[28].

Control for each PU is fully decentralized and does not need any modification in different expansion levels and operation modes. Grid-connection is possible when a grid is available.

The proposed MG solution has the following advantages.

1) It allows a bottom-up way to establish a power network. Users can start with single PU and expand the system as their demand and budget grow or interconnect the system with their neighbors'.
2) Separate local household-level bus and public dc bus allows the use of two voltage levels. The low-voltage 48 V household-level bus is safe for untrained people to use and install. High-voltage public bus keeps low distribution loss.
3) Public dc bus is isolated from each local dc bus with GCs. Reliability is improved so that failure can be isolated within the local bus range.
4) Group expansion can be achieved without interfacing converters, which reduces cost and power loss.
5) The modular design of PU and GC could significantly reduce the design cost of MG and enables mass production.
6) Fully decentralized control keeps high reliability and robustness and saves cost on communication devices.

Noticing that all PUs in one group share only one common bus, a relay is necessary at each PU's output terminal to protect devices under fault condition. And the number of PUs connected to one local bus should be limited to a reasonable value not exceeding the GC capacity to guarantee a good reliability.

The proposed MG has a bottom-up building feature that allows system growing organically as the demands grow. The feature that combines advantages of conventional SHS and central MG could significantly reduce the difficulty of developing MGs in rural developing areas.

The article is organized as follows. In Section II, the architecture of the proposed module-based MG is introduced. In Section III, detailed design of fully decentralized MG control is provided. Section IV provides simulation and experiment results to verify the analytical study. Conclusion is given in Section V.

II. Architecture of Proposed PnP MG

As shown in Fig. 1(c), the proposed PnP MG has three expansion levels—stand-alone, group expansion, and intergroup expansion. This section will introduce the proposed MG architecture by these three expansion levels.

In stand-alone mode, a single PU can operate as an SHS, providing basic energy supply. Fig. 2 shows the diagram of a single proposed PU. The PU consists of two power electronic converters: a dc–dc converter for PV generation, and a dc–dc converter for BES. Each PU is controlled by an independent digital controller.

Multiple PUs can be interconnected directly through the local dc link to provide bulk power to users as a group. Fig. 3 shows the diagram of an MG that contains multiple groups. As mentioned in Section I, direct bus interfacing could omit interfacing converters; however, the control coordination could become challenging, which will be discussed in detail in Section III.

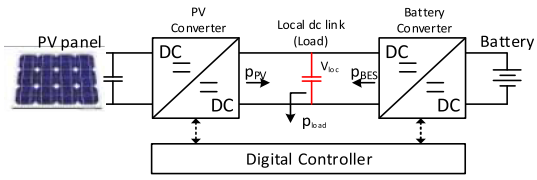

Fig. 2. Diagram of a proposed PU.

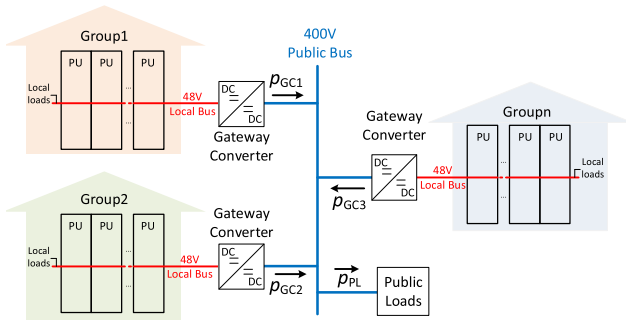

Fig. 3. Diagram of the proposed MG with intergroup expansion.

Multiple groups can be interconnected to a public network in a relatively large area to enable power exchange among households and usage of public loads. Fig. 3 shows the diagram of the proposed MG in intergroup expansion. The interconnection of groups requires interfacing converters called as GC in this article. The GC boosts the low voltage (48 V) on the group side to a high voltage (200–400 V) on the public network side, provides galvanic isolation, and controls power flow between local group and the public network. With the proposed control method, GC could compensate net load/generation differences and balance SoCs among groups automatically without communication.

Notice that, the PUs inside a group are very close to each other, where the line resistance among the PUs can be obviously neglected. For the public network, the line resistance can also be neglected to simplify the study considering the following two facts.

1) The community network is still in a relatively small scale (in a hundreds-meters range). With proper selection of conductor size and voltage level, the line resistance is very small.
2) Each GC only maintains bus voltage at its terminal with droop control, the line resistance only affects the performance of power sharing among groups. The virtual resistance in droop control is much larger than line resistance. Thus, the effect of line resistance on power sharing is also neglectable.

III. Decentralized Control Strategy for Proposed MG Module

To achieve PnP and robust operation in all expansion levels while keeping low cost and high reliability, a fully decentralized

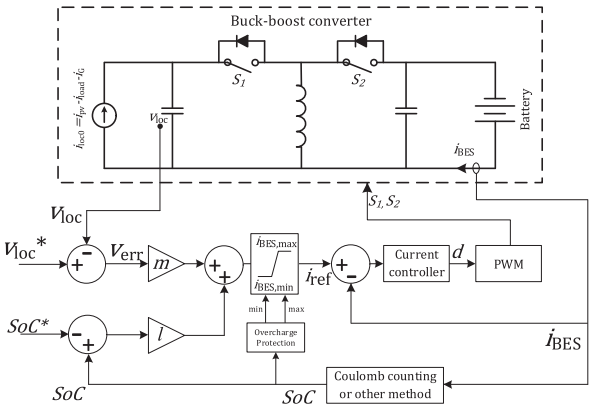

Fig. 4. Block diagram of SoC-based droop control for BES converter.

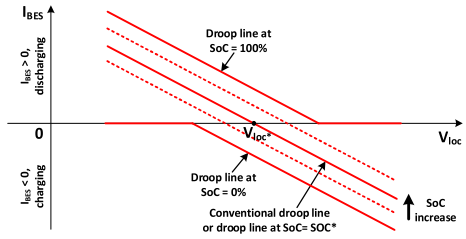

Fig. 5. Droop lines of SoC-based droop control under different SoCs.

control system independent from communication has been designed in this article. Mode transitions of each converter can be achieved seamlessly. The proposed method is developed from dc bus signaling control proposed by [27] and [28]. And new SoC self-convergence control and seamless PV mode adaptive control are integrated to the conventional dc bus signaling technology. This section introduces the detailed design and implementation of the proposed decentralized control to achieve the proposed scalable MG in a wireless and seamless manner.

A. BES Converter Control

In a regular operation scenario, the BES converter should regulate local dc bus voltage with droop control to compensate the power mismatch between PV MPPT output and load consumption. Besides voltage regulation, the BES SoCs of parallel PUs should be kept balanced to make full usage of each battery. In [29] and [30], modified droop control has been proposed to achieve BES SoC self-convergence without communication, by adjusting the droop resistance. Different from existing solutions, to accommodate dc bus signaling, this article adds a first-order term to the conventional droop control to achieve SoC self-convergence, rather than changing the droop resistance, which is important for the control coordination in the proposed MG. Fig. 4 shows the diagram of the proposed controller for BES converter. The modified droop control, which is based on *I–V* droop control, follows

$$i_{\mathrm{BES}} = m_{\mathrm{BES}} \left(V^*_{\mathrm{loc}} - v_{\mathrm{loc}}\right) + l \left(\mathrm{SoC}_{\mathrm{SoC}^*}\right) \tag{1}$$

where V^*_{loc} is the rated local bus dc link voltage and SoC^* is a reference value of SoC ramp term.

Fig. 5 shows the droop lines of the proposed modified BES droop control. Besides the conventional *I–V* droop term that output current is proportional to voltage error, it contains an SoC ramp term. With the additional term, the output current will slightly increase when BES SoC level is higher than SoC^*; the output current will slightly decrease when SoC level is lower than SoC^*. Thus, an SoC self-convergence characteristic can be created. By properly selecting parameter l, the voltage deviation can be kept in an acceptable range.

It is also shown in Fig. 4 that a saturator is added to the BES current reference. An overcharge protector provides limits for saturation stage based on information of SoC. When SoC is 0% or lower than a minimum SoC level, the current upper limit is set to zero (prevent from overdischarging); when SoC is 100%, the current lower limit is set to zero (prevent from overcharging). When the BES operation is limited by the saturator, the BES converter loses the droop characteristic. At this point, the bus voltage should be maintained by PV converter(s) (when BES is saturated to charging limit) or GC (when BES is saturated to discharging limit).

The proposed MG has to use the proposed SoC self-convergence control with a first-order SoC term rather than the conventional method as discussed in [29] and [30] due to the following reasons.

1) Some other important control parameters are selected based on the BES droop coefficient m_{BES}. The proposed method has a fixed droop coefficient rather than the conventional method adjusting the droop coefficient all the time.
2) Another important reason is the linearity, which the conventional method cannot provide. The proposed method provides a linear relationship between local voltage, local SoC, and local net generation/load, which will be used for the GC control to compensate the power mismatch and SoC unbalance among multiple groups.
3) The proposed method also takes advantage of consistency in the charging and discharging process and stable balancing speed, which is not related to charge/discharge power.

Under BES droop control, v_{loc} follows

$$v_{\mathrm{loc}} = V^*_{\mathrm{loc}} + \frac{l}{m_{\mathrm{BES}}} \left(\mathrm{SoC}^*_{\mathrm{SoC}}\right) - \frac{1}{m_{\mathrm{BES}}} i_{\mathrm{BES}} \tag{2}$$

which is used in the dc bus signaling system design.

B. PV Converter Control

In a grid-connected PV system, PV panels can always operate under MPPT control theoretically while the grid can always absorb surplus power. However, in a small off-grid system as the proposed MG, PV generation has to be able to operate under droop control when BES is fully charged. In [31], a control for PV sources with a switch choosing two control configurations was proposed, which increases system complexity. In [32], a seamless control for PV sources with an inner control loop to control *dP/dV* was proposed, which can achieve seamless mode

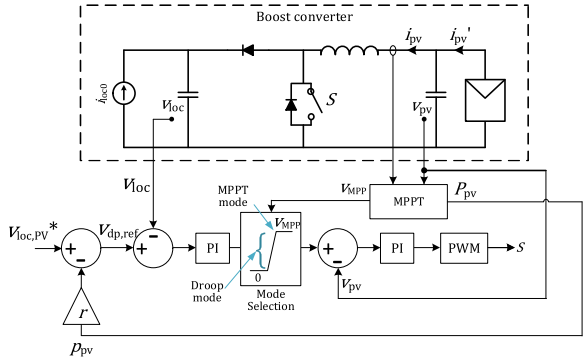

Fig. 6. Block diagram of PV converter control with seamless mode selection.

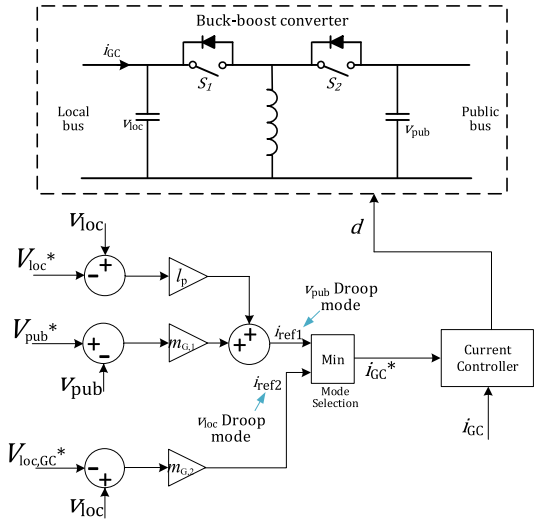

Fig. 7. Block diagram of GC control.

transition by a saturator to *dP*/*dV* reference. However accurate measurement of *dP*/*dV* could be difficult, especially for a low-cost application for rural electrification. This article proposed an alternate PV controller with seamless mode transition and more practical implementation. Fig. 6 shows the proposed mode adaptive PV converter control diagram. The inner control loop is a PV voltage loop that maintains the PV panel voltage. The outer control loop is a *V–I* droop control loop that maintains local dc link voltage, with a higher voltage reference value compared to BES droop control. The mode transition is seamless such that the saturator and local bus voltage PI controller provides the ability of automatic mode transition.

When the BES is not yet fully charged such that the local dc link voltage is well regulated by BES converter, $V_{\mathrm{dp,ref}}$ is always higher than v_{loc}, with a preselection of $V^*_{\mathrm{loc,PV}}$. The input of voltage PI controller is constantly positive, so the output of PI controller is saturated to a higher limit, which is set to MPP voltage. The inner loop will control v_{PV} to V_{MPP}, which achieves MPPT.

When PUs are fully charged or the BES current already hit the limit of $i_{\mathrm{BES,min}}$ (maximum charging current), the local dc link voltage will rise higher than $V_{\mathrm{dp,ref}}$. Then, the V_{PV} reference will decrease lower than V_{MPP}, so PV may operate at an off-MPP mode. Under PV droop control, v_{loc} follows

$$v_{\mathrm{loc}} = V^*_{\mathrm{loc,PV}} - r \cdot p_{\mathrm{PV}}. \tag{3}$$

When load increases such that $p_{\mathrm{PV}} < p_{\mathrm{load}}$, the dc link voltage will drop, V_{PV} will rise up until reaching MPP, and BES starts to discharge, maintaining the local dc link voltage.

C. GC Control

Fig. 7 shows the control diagram of GC in the proposed MG architecture. Any bidirectional dc–dc topology can be used for GC, e.g., boost, flyback, forward, dual-active-bridge, etc. And in this article, buck-boost converter is used for GC to demonstrate the general idea. As the interface between local low-voltage dc bus and public medium-voltage dc bus, the GC has two operation modes, v_{pub} control mode and v_{loc} control mode. Similar to PV mode selection, which is based on a voltage threshold, the GC mode selection uses smaller current reference from i_{ref1} (generated by public bus droop control) and i_{ref2} (generated by local bus droop control). As a result, the power direction change becomes continuous and seamless. GC and BES converter can work simultaneously under droop control establishing local dc bus voltage.

In v_{pub} control mode, with the local group operating in healthy condition, the GC will maintain the public dc bus voltage with a modified droop control, as $i_{\mathrm{ref1}} < i_{\mathrm{ref2}}$ in Fig. 7. The current reference in v_{pub} control mode is given by

$$i_{\mathrm{ref1}} = m_{\mathrm{G},1}\left(V^*_{\mathrm{pub}} - v_{\mathrm{pub}}\right) + l_{\mathrm{p}}\left(v_{\mathrm{loc}} - V^*_{\mathrm{loc}}\right). \tag{4}$$

In v_{loc} control mode, the energy stress of the local group is too high to support the public network that $i_{\mathrm{ref2}} < i_{\mathrm{ref1}}$, therefore, the GC can reduce the output power even to reversely inject power into the local group to maintain the local dc link voltage inside the acceptable level. The controller for GC in v_{loc} control mode uses simple *I–V* droop control

$$i_{\mathrm{ref2}} = m_{\mathrm{G},2}\left(v_{\mathrm{loc}} - V^*_{\mathrm{loc,GC}}\right) \tag{5}$$

where $V^*_{\mathrm{loc,GC}}$ is rated voltage for GC local bus droop control. The selection of $V^*_{\mathrm{loc,GC}}$ will be explained in detail in Section III-D.

The mode selection is based on i_{ref2} , which is actually an indicator of group energy stress. The larger i_{ref2} is, the less stressed the group is. In v_{pub} control mode, $i_{\mathrm{ref2}} > i_{\mathrm{ref1}}$, the GC will follow the public bus droop control. In v_{loc} control mode, $i_{\mathrm{ref2}} < i_{\mathrm{ref1}}$, the GC will maintain the local dc bus at a minimum level. Fig. 8 shows the droop line of local bus droop control of GC.

For selecting the parameters of GC control, an important difference is that GC could be connected to groups with different number of PUs. Thus, the control parameters of GC should be adjusted according to the number of PUs connected to local group to proportionally share power with other groups. The setting of number n can be achieved by simply using buttons or a knob on the GC, which can be done by even untrained

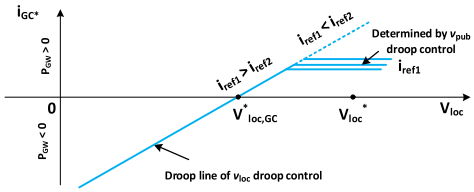

Fig. 8. Droop line of local bus droop control of GC.

people and will not spoil the PnP feature. Thus, $m_{\mathrm{G},2}$, $m_{\mathrm{G},1}$, and l_{p} should be adjusted accordingly

$$m_{\mathrm{G},1} = n \cdot m'_{\mathrm{G},1} \tag{6}$$

$$m_{\mathrm{G},2} = n \cdot m'_{\mathrm{G},2} \tag{7}$$

$$l_{\mathrm{p}} = n \cdot l'_{\mathrm{p}} \tag{8}$$

where n is the number of PUs connected to the local bus, $m'_{\mathrm{G},1}$ and $m'_{\mathrm{G},2}$ are droop coefficients per unit for local bus droop control and public bus droop control, respectively, and l'_{p} is the per unit coefficient for SoC balance among groups.

The values of $m_{\mathrm{G},1}{}'$ and $m_{\mathrm{G},2}{}'$ could follow regular droop controller design procedure, considering the acceptable range of voltage variation toward certain power variations. Specifically, to achieve same voltage regulation performance on local bus under usage-dominating mode as under storage-dominating mode, $m'_{\mathrm{G},2}$ should be equal to m_{BES}. l'_{p} should also be equal to m_{BES} to achieve automatic compensation of load/generation mismatch, which will be explained later.

Different from conventional solutions as shown in Fig. 1(a), the interfacing converter, BES converter, and PV converter can be controlled by one controller device with shared information. A challenge for GC is how to achieve power flow control and SoC balance among groups simultaneously without communicating with other devices. The proposed GC control coordinate with proposed BES droop control is as introduced in Section III-A, which naturally achieves automatic power flow control to compensate load/generation mismatch and SoC self-convergence among multiple groups.

As shown in (4), the GC v_{pub} droop control also consists of two terms, one conventional *I–V* droop control term and a first-order term reflects local voltage. Considering groups could have different numbers of PUs, (4) can be rewritten as

$$\frac{i_{\mathrm{GC}}}{n} = m'_{\mathrm{G},1}\left(V^*_{\mathrm{pub}} - v_{\mathrm{pub}}\right) + l'_{\mathrm{p}}\left(v_{\mathrm{loc}} - V^*_{\mathrm{loc}}\right) \tag{9}$$

where i_{GC} is the current of the GC on the local bus side.

All GCs are connected to the same public bus, so the first terms in (9) are same in all GCs. Thus, the circulating current to balance power and SoC is only generated from the second term

$$i_{\mathrm{GC,c,p.u.}} = l'_{\mathrm{p}}\left(v_{\mathrm{loc}} - v_{\mathrm{loc,avg}}\right) \tag{10}$$

where $i_{\mathrm{GC,c,p.u.}}$ is the per PU circulating current going through GCs. With local SoC self-convergence control proposed in Section III-A, the local bus voltage contains information of both group net load/generation and group average SoC. Put (2) into (10)

$$i_{\mathrm{GC,c,p.u.}} = \frac{l'_{\mathrm{p}}}{m_{\mathrm{BES}}}\left(i_{\mathrm{BES,avg}} - i_{\mathrm{BES}}\right) + \frac{l'_{\mathrm{p}} l}{m_{\mathrm{BES}}}\left(\mathrm{SoC}_{\mathrm{loc,avg}} - \mathrm{SoC}_{\mathrm{global,avg}}\right). \tag{11}$$

Apparently, the circulating current as in (11) consists of two parts. The first term $\frac{l'_{\mathrm{p}}}{m_{\mathrm{BES}}}(i_{\mathrm{BES,avg}} - i_{\mathrm{BES}})$ is used to provide compensation for load/generation mismatch among the groups. When $\frac{l'_{\mathrm{p}}}{m_{\mathrm{BES}}} = 1$, the first term becomes exactly the current mismatch of each PU. The second term $\frac{l'_{\mathrm{p}} l}{m_{\mathrm{BES}}}(\mathrm{SoC}_{\mathrm{loc,avg}} - \mathrm{SoC}_{\mathrm{global,avg}})$ is used to balance the SoCs among multiple groups. Make the difference between $\mathrm{SoC}_{\mathrm{loc,avg}}$ and $\mathrm{SoC}_{\mathrm{global,avg}}$ to be $\Delta\mathrm{SoC}_{\mathrm{loc,avg}}$, which can be expressed following the definition of SoC as:

$$\frac{\mathrm{d}\Delta\mathrm{SoC}_{\mathrm{loc,avg}}}{\mathrm{d}t} = -i_{\mathrm{BES}} + i_{\mathrm{BES,avg}} \tag{12}$$

Put (11) into (12) and considering $\frac{l'_{\mathrm{p}}}{m_{\mathrm{BES}}} = 1$

$$\frac{\mathrm{d}\Delta\mathrm{SoC}_{\mathrm{loc,avg}}}{\mathrm{d}t} = i_{\mathrm{GC,c,p.u.}} - l\Delta\mathrm{SoC}_{\mathrm{loc,avg}}. \tag{13}$$

Solve (13)

$$\Delta\mathrm{SoC}_{\mathrm{loc,avg}}(t) = \Delta\mathrm{SoC}_{\mathrm{loc,avg}}(0) + \frac{i_{\mathrm{GC,c,p.u.}}}{l}\left(1 - e^{-lt}\right). \tag{14}$$

Thus, the SoC difference can be converged to

$$\Delta\mathrm{SoC}_{\mathrm{loc,avg}}(\infty) = \Delta\mathrm{SoC}_{\mathrm{loc,avg}}(0) + \frac{i_{\mathrm{GC,c,p.u.}}}{l}. \tag{15}$$

From (15) it can be seen that the SoC converge performance on GCs is different from BES converters. It cannot guarantee SoC difference converging to zero but only to a certain value related to GC operating condition. Though the SoCs among groups will have differences, the trend is kept from divergence. This difference is caused by different load/generation conditions in multiple groups. Only when the net load/generation per PU of all groups are equal, $\Delta\mathrm{SoC}_{\mathrm{loc,avg}}(\infty)$ is equal to zero. Considering that the per unit net load/generation in each group would be similar in a large time scale, the SoCs among groups can be kept balanced in long term dynamically.

D. Control Coordination

As mentioned, for each group, multiple PUs are directly bus interfaced. The coordination of parallel PV converters, BES converters, and GCs is the key challenge in the proposed MG architecture. While the public dc bus control is much simple and has been studied by many researchers, this section will be more focused on the local group control coordination.

With proposed controllers for each converter, the coordination, including mode transition, power sharing, and SoC balance can be achieved simultaneously in a fully decentralized manner. As introduced above, generally, each converter in the proposed MG has two operation modes, which can be concluded as Table I. All mode transitions are based on seamless control.

TABLE I
SUMMARIZE OF CONVERTER MODES AND CRITERIA

	Mode 1	Mode 2	Mode transition criteria
BES converter	v_{loc} droop control	saturated	SoC level
PV converter	MPPT	v_{loc} droop control	v_{PV} reference saturated to V_{MPP} or not
Gateway converter	v_{pub} droop control	v_{loc} droop control	Comparing i_{ref1} and i_{ref2}

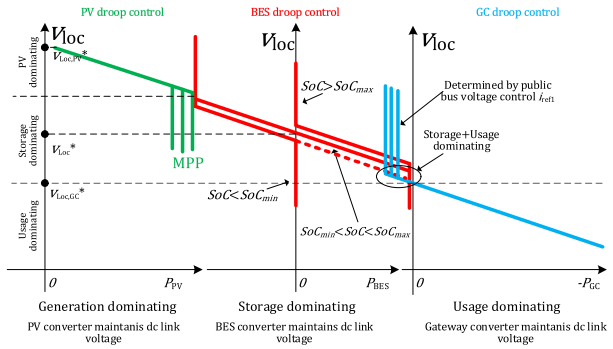

Fig. 9. Coordination of local dc bus droop control.

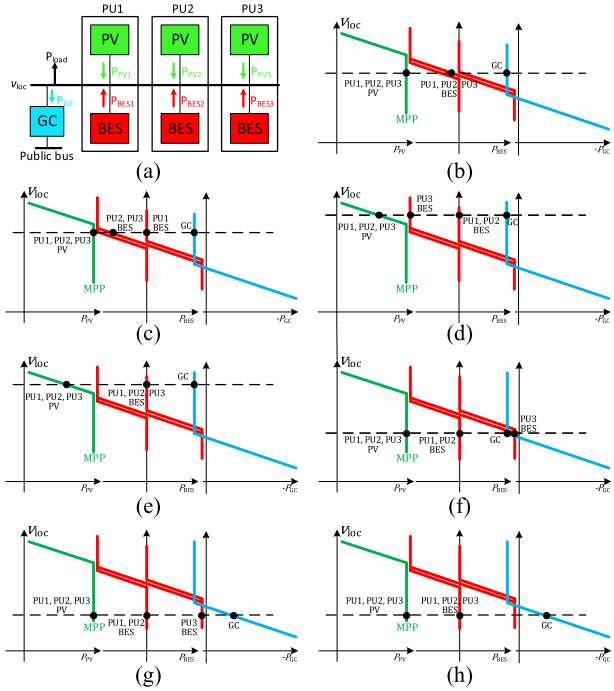

Fig. 10. Typical operating modes of a group in proposed MG. (a) Group diagram. (b) Storage-dominating mode with all batteries available. (c) Storage-dominating mode (PU1 drained). (d) PV-dominating mode (PU1 and PU2 fully charged, PU3 at charging current limit). (e) PV-dominating mode (all PUs fully charged). (f) Storage-dominating mode + usage-dominating mode (PU1 and PU2 drained). (g) Usage-dominating mode (PU1 and PU2 drained and PU3 at discharging current limit). (h) Usage-dominating mode (all PUs drained).

Besides the modes of each converter, the overall system operation can be put into three modes. Fig. 9 demonstrates the coordination of PV, BES, and GC droop control. Based on which part is dominating droop control, the three modes are generation-dominating mode, storage-dominating mode, and usage-dominating mode [27]. The local dc link voltage v_{loc} works as an indicator of operation mode. To achieve wireless and seamless mode transition, the parameters for each converter controller should be carefully designed.

PV should operate under MPPT control whenever BES can maintain v_{loc}. By (2) and (3), the parameters should satisfy

$$V^*_{\text{loc,PV}} - r \cdot p_{\text{PV,max}} \geq V^*_{\text{loc}} + \frac{l}{m_{\text{BES}}}(\text{SoC}_{\max} - \text{SoC}^*) - \frac{1}{m_{\text{BES}}} I_{\text{BES,min}}. \tag{16}$$

And noticing that the power range of PV is dependent on MPP power, a voltage gap between PV droop control and BES droop control is inevitable, which will not have any negative influence on the system stability or reliability.

Different from having a relatively clear boundary between PV-dominating mode and storage-dominating mode, the storage-dominating mode can have an overlapping area with usage-dominating mode. It is allowed to have v_{loc} under droop control simultaneously from BES and GC. This overlap can reduce the stress of local BES at low SoC level and make the mode transition process smoother. The overlap is generated naturally from the selection of parameter $V^*_{\text{loc,GC}}$. Reaching the local voltage reaching $V^*_{\text{loc,GC}}$ means the BESs cannot further provide any power. Any further decrease of local bus voltage should be compensated by injecting power from GC. Thus, it makes sense to set GC power equal to zero at $V^*_{\text{loc,GC}}$ and $V^*_{\text{loc,GC}}$ should follow

$$V^*_{\text{loc,GC}} = V^*_{\text{loc}} - \frac{1}{m_{\text{BES}}} I_{\text{BES,max}}. \tag{17}$$

The width of overlapping is determined by i_{ref1}, which is generated from public bus voltage droop control.

Fig. 10 shows typical operating scenarios of a group consisting of three PUs and one GC under different operation modes. Fig. 10(a) shows the group connection diagram. Fig. 10(b) shows a regular condition that all PUs are available, batteries can absorb or release energy to maintain the local bus voltage with droop control; the system is under storage-dominating mode. The operating points of three BES converters are on the droop line, three PV converters are under MPPT control, and GC can be regarded as load feeding power into public dc link. In Fig. 10(c), though PU1 is fully charged that the operating point is saturated to zero current, the other PUs can still absorb surplus power, the group still operates under storage-dominating mode. In Fig. 10(d), PU1 and PU2 are fully charged and PU3 hits the maximum charging power, all PUs cannot further absorb surplus power. Thus, v_{loc} rises and PV converters operate under droop control to maintain v_{loc}, which makes the system in PV-dominating mode. In Fig. 10(e), all PUs are fully charged and the group is kept in PV-dominating mode, until PV output cannot meet the load consumption, batteries will start to discharge and change back to storage-dominating mode. In Fig. 10(f), PU1 and PU2 BESs are drained and saturated to zero output power, though both PV are

TABLE II
SIMULATION AND EXPERIMENT PARAMETERS

Item	Symbol	Value	Item	Symbol	Value
Rated local dc bus voltage	V^*_{loc}	48 V	Max discharging current	$i_{\text{BES,max}}$	4.2 A
Droop reference of PV converter	$V^*_{\text{loc,PV}}$	52 V	Max charging current	$i_{\text{BES,min}}$	-2.0 A
Droop reference of GC	$V^*_{\text{loc,GC}}$	44 V	BES v_{loc} droop coefficient	m_{BES}	1
Rated Public dc bus voltage	V^*_{pub}	200 V	BES SoC coefficient	l	0.02
BES voltage	V_{bat}	48 V	PV maximum power	$P_{\text{PV,max}}$	100 w
BES capacity	C_{bat}	10 Wh	PV droop coefficient	r	0.01
maximum SoC	$SoC_{\max}$	100 %	GC v_{pub} droop coefficient	$m'_{G,1}$	0.1/unit
minimum SoC	$SoC_{\min}$	30 %	GC v_{loc} droop coefficient	$m'_{G,2}$	1/unit
SoC^*	SoC^*	50 %	Group SoC coefficient	l_p	1/unit
Local bus capacitance	C_{loc}	660 μF/unit			

under MPPT control, v_{loc} is at a relatively low level due to the high load. GC operates under droop control with reduced power consumption. The system v_{loc} is dominated by both storage and usage. In Fig. 10(g), PU1 and PU2 are still drained, and PU3 BES is saturated to its maximum output power, BES losses the ability of v_{loc} control. Only GC operates under droop control. The system is under usage-dominating mode. Fig. 10(h) is similar to Fig. 10(g), but with all PU BESs drained. GC operates under droop control. The system is still under usage-dominating mode.

With the proposed control system design, with a certain v_{loc}, a unique operating point can be determined for each converter in the group. In all operating scenarios and expansion levels, the system can be kept stable and robust. Therefore, a true PnP feature can be realized with low cost and high reliability.

IV. SIMULATION AND EXPERIMENTAL STUDY

A. Simulation Study

Simulations based on PLECS are performed to evaluate the proposed MG architecture and the fully decentralized control technique. Table II shows the parameters used in simulation.

Fig. 11 shows the simulation results of a group consisting of three PUs, where Fig. 11(a) shows the whole scope and Fig. 11(b)–(e) shows the zoomed-in waveforms during transients. In $t_0 - t_1$, all BESs of three PUs are under droop control and all PVs are under MPPT control (with different MPP power). At t_1, BES of PU1 is fully charged and is no longer under droop control. In $t_1 - t_2$, BESs of PU2 and PU3 can still absorb surplus power to maintain $v_{\text{loc}}$with droop control to a little higher value due to the higher charging current on each BES. At t_2, BES of PU2 also gets fully charged. In $t_2 - t_3$, solely PU3 BES cannot absorb all the surplus power and is saturated to the maximum charging power. The increase of v_{loc} changes PV converters from MPPT control to droop control which keeps v_{loc} from increasing further, and PVs can evenly share the power. At t_3, BES of PU3 also gets fully charged. PVs further reduce their output with droop control to maintain v_{loc}. At t_4, a load step change from 100 to 400 W happens, such that all PVs increase their outputs to

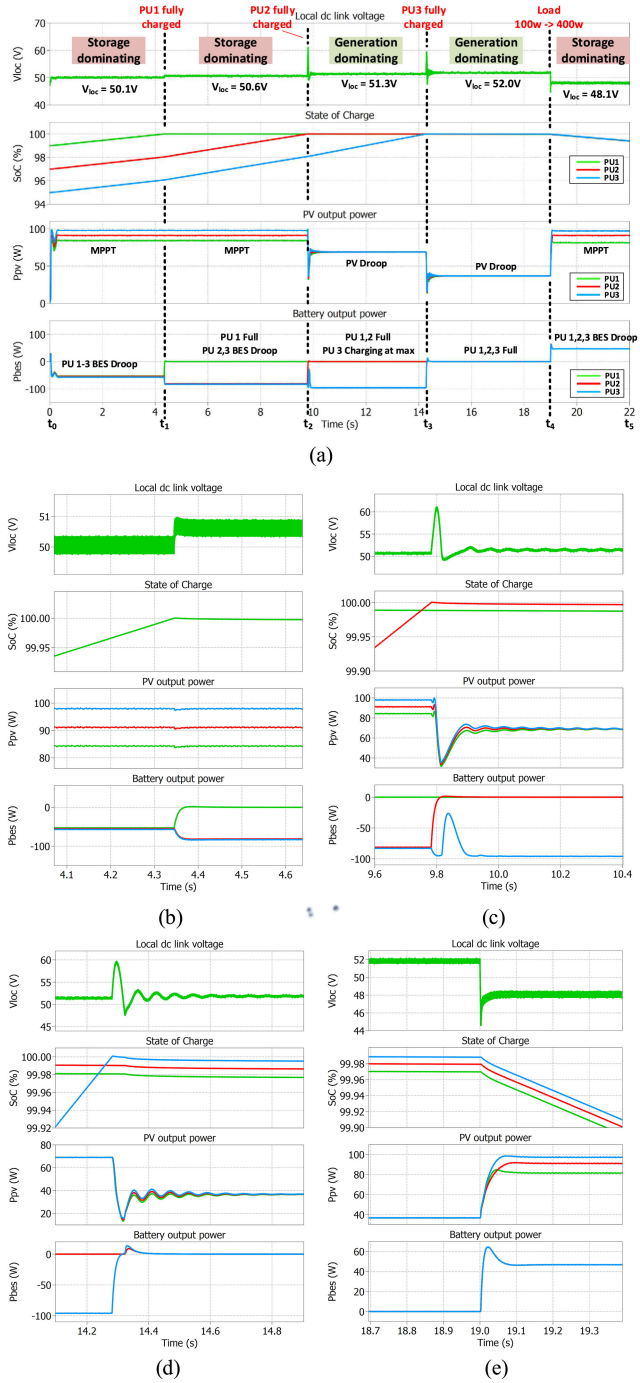

Fig. 11. Simulation results of a group consisting of three PUs. (a) Operation with group mode transitions. (b) Zoomed-in waveforms at time t_1. (c) Zoomed-in waveforms at time t_2. (d) Zoomed-in waveforms at time t_3. (e) Zoomed-in waveforms at time t_4.

MPP but still cannot meet the load need. BESs start to discharge and take back droop control.

It can be seen that when BES takes over the droop control, e.g., Fig. 11(b) and (e), the transient is much faster (shorter settling time and smaller overshoot) than that of PV taking over droop control, e.g., Fig. 11(c) and (d). It can be explained by the fact that BES converter uses *I–V* droop control, as shown in Fig. 4,

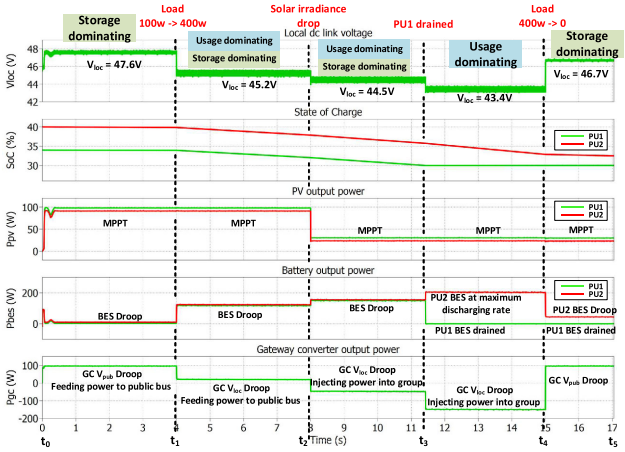

Fig. 12. Simulation result of GC mode transitions.

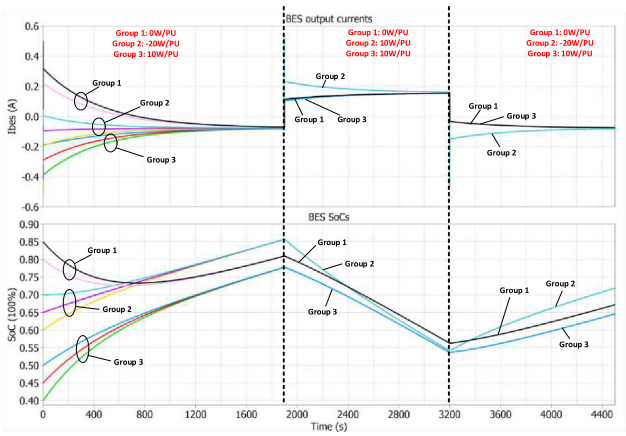

Fig. 13. Simulation result showing power sharing and SoC balance among BESs inside a group and among groups.

which has the nature of better transient performance than that of *V–I* droop control used by PV converter, as shown in Fig. 6 [33]. At the same time, the $v_{\rm loc}$ PI controller of PV converter has to have a lower control bandwidth to guarantee a stable inner $v_{\rm PV}$ loop, which could further deteriorate $v_{\rm loc}$ transient performance. With proper design of parameters and local bus capacitance, the transient can be kept in an acceptable range as shown in the simulation result (settling time 0.2 s, overshoot 10 V).

Fig. 12 shows the simulation result of a group consisting of two PUs and connected to the public bus with a GC. The simulation result shows GC operation mode change between $v_{\rm pub}$ control mode and $v_{\rm loc}$ control mode and the case $v_{\rm loc}$ is regulated by both BES and GC. In $t_0 - t_1$, BESs of two PUs are under droop control and PVs are under MPPT control. GC is working, feeding power into the public bus, of which, the power is determined by $v_{\rm pub}$ droop control. At t_1, a load step change from 100 to 400 W happens. In $t_1 - t_2$, both BESs are under droop control with increased output power. Reduced $v_{\rm loc}$ makes GC also under $v_{\rm loc}$ droop control so that the power drained from local bus is reduced. At t_2, a solar irradiance drop happens. In $t_2 - t_3$,$v_{\rm loc}$ is still maintained by BESs and GC. BESs' output power is further increased. GC output power is further decreased to negative and start to inject power into the local bus. At t_3, PU1 is drained and PU2 BES hits the maximum output power. In $t_3 - t_4$, only GC maintains $v_{\rm loc}$ with droop control. At t_4, the load is reduced to 0 from 400 W. $v_{\rm loc}$ rises to a higher value and GC changes back to $v_{\rm pub}$ control. PU2 BES maintains $v_{\rm loc}$ while PU1 is still drained such that it cannot provide any power. Notice that both BES and GC droop control are *I–V* droop control which has a high control bandwidth. As a result, all transients in Fig. 12 are smooth and fast.

Fig. 13 shows the simulation result of a case consisting of three groups, where Group 1 has two PUs, Group 2 has three PUs, and Group 3 has three PUs. As shown in Fig. 13, all PUs start with different SoC, and net load are different in the three groups with two transients of net load step change in Group 2 at 1800 and 3200 s. In this test case, the GCs are under $v_{\rm pub}$ control mode to demonstrate power sharing and SoC balancing ability among groups, due to the fact that SoC balancing and power sharing among groups are only considered under GC $v_{\rm pub}$ control mode. First, from the result, with proposed SoC self-convergence control, the SoCs inside a group converge fast to a well-balanced state, as well as the current sharing. Second, among multiple groups, as analyzed by mathematical derivations (9)–(15), the SoCs of the three groups are kept from divergence though with a steady-state SoC difference due to different net load/generation conditions which agrees with (15). And the net load/generation mismatch in the different groups are compensated as the BES output powers are well shared by each BES in all groups, with the proposed control design and parameter selection, as explained by (11).

B. Experiment Verification

The proposed MG architecture has been verified by experimental prototypes, of which the setup is shown in Fig. 14. An MG system with two PUs and one GC is tested. The verification focuses more on the group operation. The public bus is emulated as a voltage source with a battery. Each PU is controlled by a TI F28379d DSP. Parameters are set the same as Table II.

Fig. 15(a) and (b) shows the system SoC self-convergence characteristic in the charging and discharging process, respectively. SoC waveforms are generated by MATLAB with measured information of BES currents. It can be seen that the BES with higher SoC always provides higher current. A converging trend of two BES SoCs can be observed in both cases. Besides that, with the change of system overall SoC, a change on the local bus voltage $v_{\rm loc}$ can also be observed, which can be used for GC to estimate local group average SoC.

Fig. 16 shows the operation of a stand-alone PU showing PV-BES droop coordination. In $t_0 - t_1$, BES maintains $v_{\rm loc}$ with droop control and PV operates at MPP. At t_1, BES is fully charged, and BES charging current is saturated to zero; PV converter changes to droop control and maintains $v_{\rm loc}$ at a higher level with reduced PV output power. At t_2, solar irradiance is reduced. While the PV converter is still under droop control, the output power remains the same but closer to MPP with increased

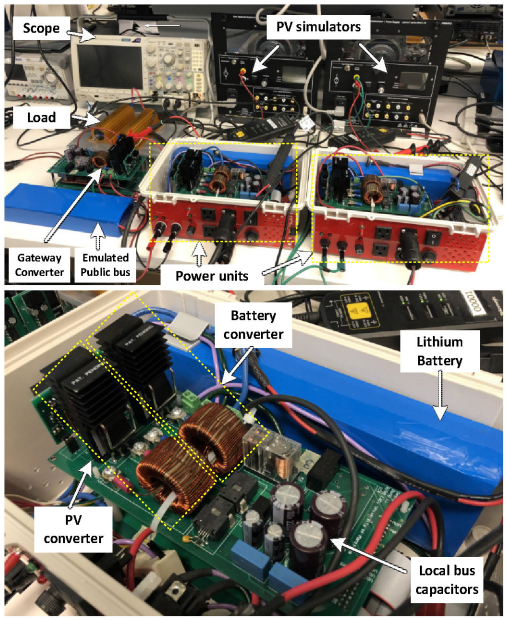

Fig. 14. Experiment setup.

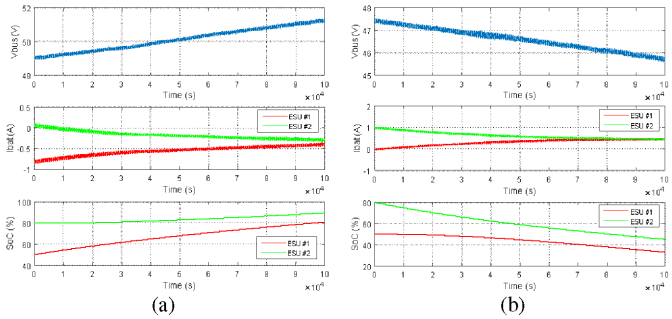

Fig. 15. Experimental waveforms of SoC self-convergence inside a group during (a) charging and (b) discharging.

$v_{\rm PV}$. At t_3, solar irradiance is further reduced. PV converter increases $v_{\rm PV}$ till it reaches MPP, but the MPP power cannot compensate the load. BES starts to discharge and maintains $v_{\rm loc}$ with droop control. At t_4, solar irradiance is reduced to zero. BES can still maintain $v_{\rm loc}$ with higher output power. Fig. 16(b) illustrates the operating points of PV during mode transitions.

Fig. 17 shows the operation of a group consisting of two PUs showing PV-BES droop coordination. The two PV simulators use different PV curves with different MPP power. In $t_0 - t_1$, PV converters operate at each MPP, and BESs maintain $v_{\rm loc}$ with droop control and equally share the power. At t_1, PU1 BES is fully charged; PU2 BES can still absorb all the surplus power with droop control; PV converters are kept at MPPT control. At t_2, PU2 BES is also fully charged so that both BESs cannot absorb any surplus power; PV converters change to droop control. At t_3, solar irradiance is significantly reduced on PV1, PV converters increase their $v_{\rm PV}$ to maintain the output power. At t_4, solar irradiance is also reduced on PV2, PV converters can

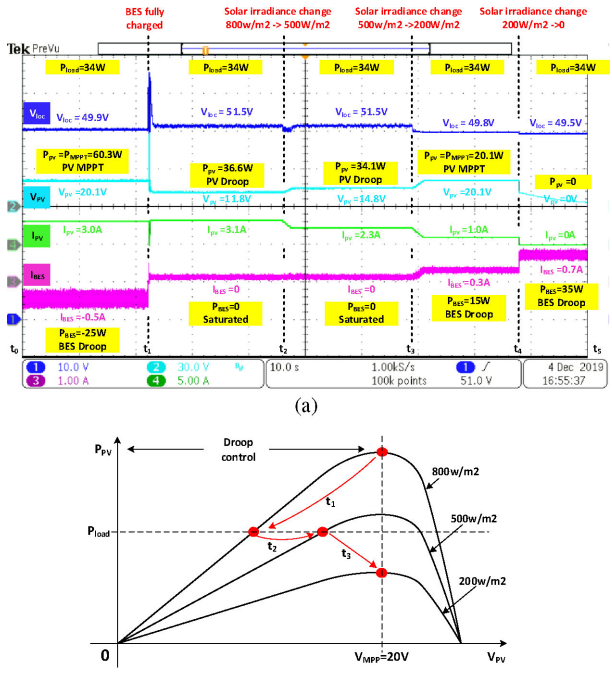

Fig. 16. Experimental results of a stand-alone PU showing PV-BES droop control coordination. (a) Waveforms. (b) PV operating points.

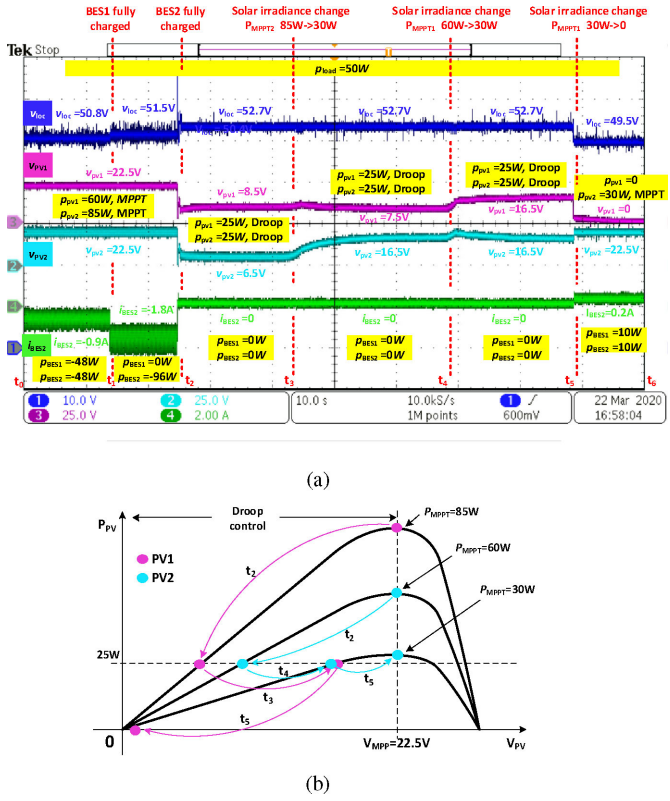

Fig. 17. Experimental waveforms of a group consisting of two PUs showing PV-BES droop coordination. (a) Waveforms. (b) PV operating points.

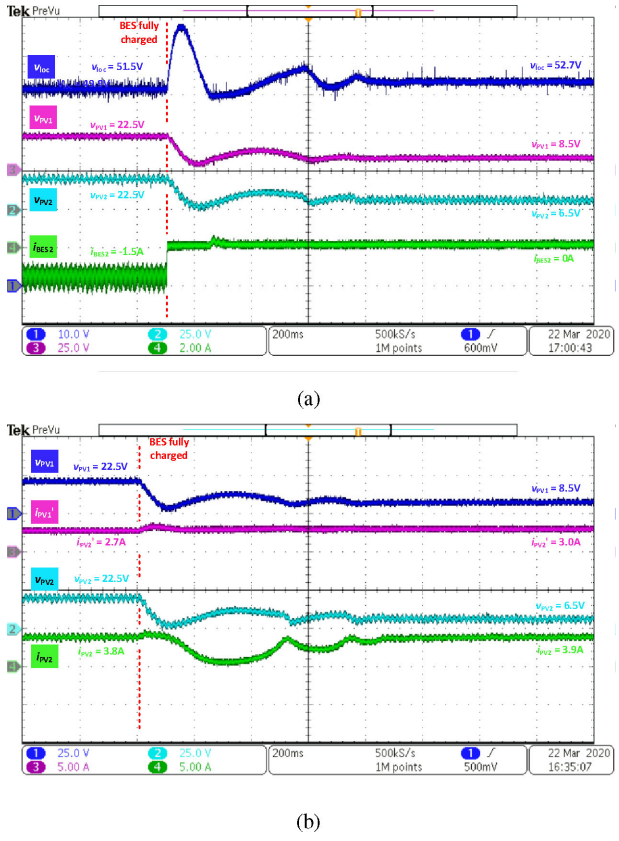

Fig. 18. Experimental waveforms of transient where both BESs get fully charged and PV converters change to droop control with $P_{\rm load} = 50\,{\rm W}$, $P_{\rm MPPT1} = 60\,{\rm W}$, and $P_{\rm MPPT2} = 85\,{\rm W}$, where (a) local bus voltage, PV panel voltages, and BES current, and (b) PV panel voltages and currents.

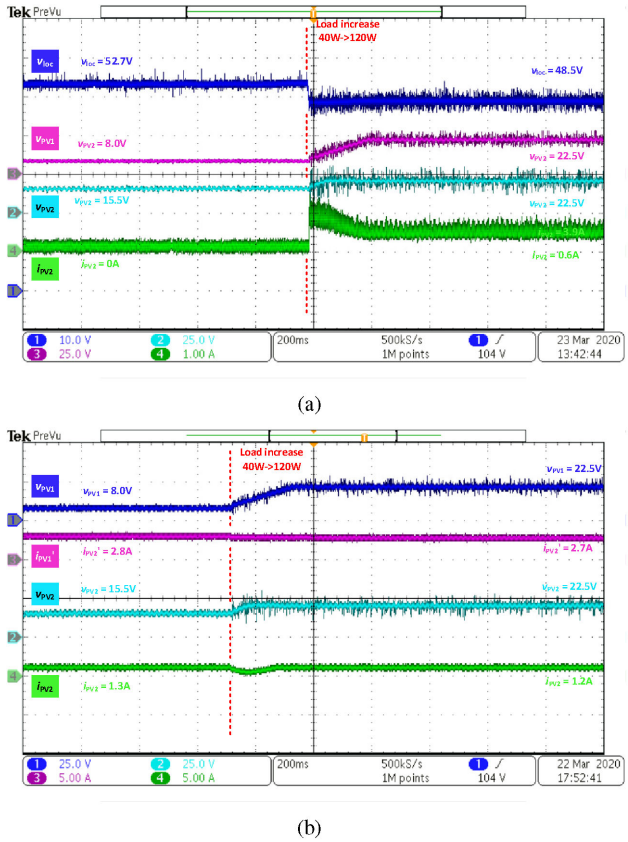

Fig. 19. Experimental waveforms of transient where load step increases by 80 W and PV converters change back to MPPT control with $P_{\rm MPPT1} = 60\,{\rm W}$ and $P_{\rm MPPT2} = 25\,{\rm W}$, where (a) local bus voltage, PV panel voltages, and one BES current, and (b) PV panel voltages and currents.

still maintain dc link voltage well with equally shared power. At t_5, PV1 is completely shut down, PV2 increase its power till reaching MPP, BESs start to discharge to maintain $v_{\rm loc}$ at lower level with droop control. Fig. 17(b) shows, in detail, how the PV operating points move on two different PV curves during the experiment. In storage-dominating mode, each PV can track its own MPP. In generation-dominating mode, two PVs can equally share the power.

Fig. 18 shows the zoomed-in waveforms of the transient from storage-dominating mode to generation-dominating mode. Fig. 19 shows the zoomed-in waveforms of the transient from generation-dominating mode back to generation-dominating mode. It can be seen that the transient of the former one has a much longer settling time and overshoot, due to the nature PV characteristic and *V–I* droop control. With a proper design of bus capacitance, the overshoot can be limited within an acceptable range.

Fig. 20 shows the experimental waveforms of coordination of PU and GC $v_{\rm loc}$ droop control. One PU and one GC are used to verify the BES-GC coordination. Public bus is emulated using a battery as constant voltage source and $i_{\rm ref1}$ is set to 1 A. In $t_0 - t_1$, BES with PV output power can well manage the load of 115 W, maintaining $v_{\rm loc}$ at an acceptable level such that GC can inject 1 A as given by reference $i_{\rm ref1}$. At t_1, load step changes to

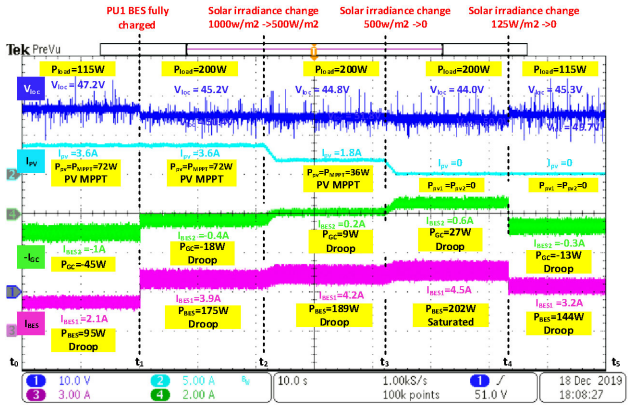

Fig. 20. Experimental waveforms of a PU and a GC showing BES-GC droop coordination.

200 W; $v_{\rm loc}$ drops to 45.2 V; both BES and GC are under droop control such that GC reduces the power injected into public bus to 0.4 A. At t_2, solar irradiance change reduces the PV output power; BES increases its output power and GC further reduce its power consumption till injecting power into local group with 0.2 A. At t_3, PV output power reduces to zero; BES operates at maximum discharging current; only GC is under droop control to

maintain $v_{\rm loc}$ at a lower level (44 V). At t_4, the load is reduced to 115 W; BES output is reduced and maintains $v_{\rm loc}$ at a relatively higher level with GC.

V. Conclusion

In this article, a module-based PnP MG is proposed with fully decentralized control. The proposed MG is based on PnP modules, namely, PUs and GC. Each PU can work as a stand-alone unit, and with the proposed decentralized control technique, multiple PUs can be put into a group to scale up the system capacity in an *ad hoc* and PnP manner. Groups can be further interconnected through a public bus with GC. Control of each converter just requires local information while power sharing, SoC balancing, and mode adaption can be achieved simultaneously in a communicationless manner. The proposed architecture allows people to organically develop power networks in a bottom-up way with PnP modules, which is suitable for electrification in rural areas. The performance of the proposed MG and control method is studied analytically and verified by simulation and experimental tests. The results show that, with the proposed method, an *ad hoc* low-cost MG with multilayer expandability can be achieved while keeping high reliability and robustness.

Acknowledgment

The authors would like to thank the competition committee and judges of IEEE Empower a Billion Lives for providing valuable comments and financial support during the regional and global final competition.

References

[1] World Energy Outlook, "Energy access outlook," 2017. [Online]. Available: https://webstore.iea.org/weo-2017-special-report-energy-access-outlook

[2] M. Nasir, H. A. Khan, N. A. Zaffar, J. C. Vasquez, and J. M. Guerrero, "Scalable solar DC microgrids: On the path to revolutionizing the electrification architecture of developing communities," *IEEE Electrific. Mag.*, vol. 6, no. 4, pp. 63–72, Dec. 2018.

[3] M. Nasir, H. A. Khan, A. Hussain, L. Mateen, and N. A. Zaffar, "Solar PV-based scalable DC microgrid for rural electrification in developing regions," *IEEE Trans. Sustain. Energy*, vol. 9, no. 1, pp. 390–399, Jan. 2018.

[4] A. Werth, N. Kitamura, and K. Tanaka, "Conceptual study for open energy systems: Distributed energy network using interconnected DC nanogrids," *IEEE Trans. Smart Grid*, vol. 6, no. 4, pp. 1621–1630, Jul. 2015.

[5] H. Kakigano, Y. Miura, and T. Ise, "Distribution voltage control for DC microgrids using fuzzy control and gain-scheduling technique," *IEEE Trans. Power Electron.*, vol. 28, no. 5, pp. 2246–2258, May 2013.

[6] T. Dragičević, X. Lu, J. C. Vasquez, and J. M. Guerrero, "DC microgrids—Part I: A review of control strategies and stabilization techniques," *IEEE Trans. Power Electron.*, vol. 31, no. 7, pp. 4876–4891, Jul. 2016.

[7] A. P. N. Tahim, D. J. Pagano, E. Lenz, and V. Stramosk, "Modeling and stability analysis of islanded DC microgrids under droop control," *IEEE Trans. Power Electron.*, vol. 30, no. 8, pp. 4597–4607, Aug. 2015.

[8] S. Moayedi and A. Davoudi, "Distributed tertiary control of DC microgrid clusters," *IEEE Trans. Power Electron.*, vol. 31, no. 2, pp. 1717–1733, Feb. 2016.

[9] A. M. Jadhav, N. R. Patne, and J. M. Guerrero, "A novel approach to neighborhood fair energy trading in a distribution network of multiple microgrid clusters," *IEEE Trans. Ind. Electron.*, vol. 66, no. 2, pp. 1520–1531, Feb. 2019.

[10] Z. Wang, F. Liu, Y. Chen, S. H. Low, and S. Mei, "Unified distributed control of stand-alone DC microgrids," *IEEE Trans. Smart Grid*, vol. 10, no. 1, pp. 1013–1024, Jan. 2019.

[11] C. Tu, F. Xiao, Z. Lan, Q. Guo, and Z. Shuai, "Analysis and control of a novel modular-based energy router for DC microgrid cluster," *IEEE J. Emerg. Sel. Topics Power Electron.*, vol. 7, no. 1, pp. 331–342, Mar. 2019.

[12] L. Meng *et al.*, "Review on control of DC microgrids and multiple microgrid clusters," *IEEE J. Emerg. Sel. Topics Power Electron.*, vol. 5, no. 3, pp. 928–948, Sep. 2017.

[13] A. Werth *et al.*, "Peer-to-peer control system for DC microgrids," *IEEE Trans. Smart Grid*, vol. 9, no. 4, pp. 3667–3675, Jul. 2018.

[14] V. Nasirian, S. Moayedi, A. Davoudi, and F. L. Lewis, "Distributed cooperative control of DC microgrids," *IEEE Trans. Power Electron.*, vol. 30, no. 4, pp. 2288–2303, Apr. 2015.

[15] M. Nasir, Z. Jin, H. A. Khan, N. A. Zaffar, J. C. Vasquez, and J. M. Guerrero, "A decentralized control architecture applied to DC nanogrid clusters for rural electrification in developing regions," *IEEE Trans. Power Electron.*, vol. 34, no. 2, pp. 1773–1785, Feb. 2019.

[16] P. A. Madduri, J. Poon, J. Rosa, M. Podolsky, E. A. Brewer, and S. R. Sanders, "Scalable DC microgrids for rural electrification in emerging regions," *IEEE J. Emerg. Sel. Topics Power Electron.*, vol. 4, no. 4, pp. 1195–1205, Dec. 2016.

[17] S. Liptak, M. Miranbeigi, S. Kulkarni, R. Jinsiwale, and D. Divan, "Self-organizing nanogrid (SONG)," in *Proc. IEEE Decentralized Energy Access Solutions Workshop*, Atlanta, GA, USA, 2019, pp. 206–212.

[18] L. Meng *et al.*, "Flexible system integration and advanced hierarchical control architectures in the Microgrid Research Laboratory of Aalborg University," *IEEE Trans. Ind. Appl.*, vol. 52, no. 2, pp. 1736–1749, Mar./Apr. 2016.

[19] Y. Han, X. Ning, P. Yang, and L. Xu, "Review of power sharing, voltage restoration and stabilization techniques in hierarchical controlled DC microgrids," *IEEE Access*, vol. 7, pp. 149202–149223, 2019.

[20] Q. Shafiee, T. Dragičević, J. C. Vasquez, and J. M. Guerrero, "Hierarchical control for multiple DC-microgrids clusters," *IEEE Trans. Energy Convers.*, vol. 29, no. 4, pp. 922–933, Dec. 2014.

[21] X. Lu, J. M. Guerrero, K. Sun, and J. C. Vasquez, "An improved droop control method for DC microgrids based on low bandwidth communication with DC bus voltage restoration and enhanced current sharing accuracy," *IEEE Trans. Power Electron.*, vol. 29, no. 4, pp. 1800–1812, Apr. 2014.

[22] F. Guo, L. Wang, C. Wen, D. Zhang, and Q. Xu, "Distributed voltage restoration and current sharing control in islanded DC microgrid systems without continuous communication," *IEEE Trans. Ind. Electron.*, vol. 67, no. 4, pp. 3043–3053, Apr. 2020.

[23] Q. Li, F. Chen, M. Chen, J. M. Guerrero, and D. Abbott, "Agent-based decentralized control method for islanded microgrids," *IEEE Trans. Smart Grid*, vol. 7, no. 2, pp. 637–649, Mar. 2016.

[24] N. L. Diaz, T. Dragičević, J. C. Vasquez, and J. M. Guerrero, "Intelligent distributed generation and storage units for DC microgrids—A new concept on cooperative control without communications beyond droop control," *IEEE Trans. Smart Grid*, vol. 5, no. 5, pp. 2476–2485, Sep. 2014.

[25] X. Li *et al.*, "Observer-based DC voltage droop and current feed-forward control of a DC microgrid," *IEEE Trans. Smart Grid*, vol. 9, no. 5, pp. 5207–5216, Sep. 2018.

[26] M. Mokhtar, M. I. Marei, and A. A. El-Sattar, "An adaptive droop control scheme for DC microgrids integrating sliding mode voltage and current controlled boost converters," *IEEE Trans. Smart Grid*, vol. 10, no. 2, pp. 1685–1693, Mar. 2019.

[27] Y. Gu, X. Xiang, W. Li, and X. He, "Mode-adaptive decentralized control for renewable DC microgrid with enhanced reliability and flexibility," *IEEE Trans. Power Electron.*, vol. 29, no. 9, pp. 5072–5080, Sep. 2014.

[28] K. Sun, L. Zhang, Y. Xing, and J. M. Guerrero, "A distributed control strategy based on DC bus signaling for modular photovoltaic generation systems with battery energy storage," *IEEE Trans. Power Electron.*, vol. 26, no. 10, pp. 3032–3045, Oct. 2011.

[29] X. Lu, K. Sun, J. M. Guerrero, J. C. Vasquez, and L. Huang, "Double-quadrant state-of-charge-based droop control method for distributed energy storage systems in autonomous DC microgrids," *IEEE Trans. Smart Grid*, vol. 6, no. 1, pp. 147–157, Jan. 2015.

[30] X. Lu, K. Sun, J. M. Guerrero, J. C. Vasquez, and L. Huang, "State-of-charge balance using adaptive droop control for distributed energy storage systems in DC microgrid applications," *IEEE Trans. Ind. Electron.*, vol. 61, no. 6, pp. 2804–2815, Jun. 2014.

[31] A. Elrayyah, Y. Sozer, and M. E. Elbuluk, "Modeling and control design of microgrid-connected PV-based sources," *IEEE J. Emerg. Sel. Topics Power Electron.*, vol. 2, no. 4, pp. 907–919, Dec. 2014.

[32] H. Cai, J. Xiang, and W. Wei, "Decentralized coordination control of multiple photovoltaic sources for DC bus voltage regulating and power sharing," *IEEE Trans. Ind. Electron.*, vol. 65, no. 7, pp. 5601–5610, Jul. 2018.

[33] H. Wang, M. Han, R. Han, J. M. Guerrero, and J. C. Vasquez, "A decentralized current-sharing controller endows fast transient response to parallel DC–DC converters," *IEEE Trans. Power Electron.*, vol. 33, no. 5, pp. 4362–4372, May 2018.

Dong Li (Student Member, IEEE) received the B.Sc. degree in electrical engineering and B.Admin. dual degrees from Tianjin University, Tianjin, China, in 2015. He is currently working toward the Ph.D. degree in electrical engineering with the University of Manitoba, Winnipeg, MB, Canada.

He is currently a Research Assistant with the Laboratory of Renewable-Energy Interface and Grid Automation, Department of Electrical and Computer Engineering, University of Manitoba. His research interests include renewable energy interfaces, modular power electronic converters, and microgrid technologies.

Carl Ngai Man Ho (Senior Member, IEEE) received the B.Eng. and M.Eng. double degrees and the Ph.D. degree in electronic engineering from the City University of Hong Kong, Hong Kong, in 2002 and 2007, respectively.

From 2002 to 2003, he was a Research Assistant with the City University of Hong Kong. From 2003 to 2005, he was an Engineer with e.Energy Technology Ltd., Hong Kong. In 2007, he joined ABB Switzerland, Zurich, Switzerland. He has been appointed as Principal Scientist and led a research project team at ABB to develop solar inverter technologies. In October 2014, he joined the University of Manitoba, Winnipeg, MB, Canada, where he is currently an Associate Professor and Canada Research Chair in efficient utilization of electric power. He established the Renewable-Energy Interface and Grid Automation (RIGA) Lab, University of Manitoba, to carry out research on microgrid technologies, renewable energy interfaces, real-time digital simulation technologies, and demand-side control methodologies.

Dr. Ho was the recipient of the Second Place Winner for 2018 Prize Paper Awards of the IEEE TRANSACTIONS ON POWER ELECTRONICS (TPEL) and the Associate Editor Awards of the IEEE JOURNAL OF EMERGING AND SELECTED TOPICS IN POWER ELECTRONICS (JESTPE) in 2018 and 2020. He is currently an Associate Editor for the IEEE TPEL and IEEE JESTPE.